

Shadowing Effects on Particle and Transverse Energy Production*

V. Emel'yanov^a, A. Khodinov^a, S. R. Klein^b and R. Vogt^{b,c}

^aMoscow State Engineering Physics Institute (Technical University), Kashirskoe Ave. 31, Moscow, 115409, Russia

^bLawrence Berkeley National Laboratory, Berkeley, CA 94720, USA

^cPhysics Department, University of California, Davis, CA 95616, USA

The effect of shadowing on the early state of ultrarelativistic heavy ion collisions and transverse energy production is discussed. Results are presented for RHIC Au+Au collisions at $\sqrt{s_{NN}} = 200$ GeV and LHC Pb+Pb collisions at $\sqrt{s_{NN}} = 5.5$ TeV.

The proton and neutron structure functions are modified in the nuclear environment [1], referred to here as shadowing. In most shadowing models, such as gluon recombination, the structure function modifications should be correlated with the local nuclear density. The E745 experiment studied the spatial distribution of structure functions with νN interactions in emulsion [2]. They found evidence of a spatial dependence but could not determine the form. The spatial dependence of shadowing is reflected in particle production as a function of impact parameter, b , which may be inferred from the total transverse energy, E_T , produced in a heavy ion collision [3].

At RHIC and LHC perturbative QCD processes are expected to be an important component of the total particle production. In particular, at early times, $\tau_i \sim 1/p_T \leq 1/p_0 \sim 0.1$ fm for $p_0 \sim 2$ GeV, semihard production of low p_T minijets sets the stage for further evolution [4].

The average transverse energy of minijet production is proportional to the initial energy density and is the hard scattering contribution to the average total transverse energy. It is calculated within a specific detector acceptance $\epsilon(y)$. At leading order, the average transverse energy for a given minijet flavor, f , as a function of impact parameter is

$$\begin{aligned} \bar{E}_T^f(b) &= \frac{d\sigma^f \langle E_T^f \rangle}{d^2b} = K_{\text{jet}} \int d^2r dp_T^2 dy_2 dy dz dz' \sum_{\substack{ij= \\ (kl)}} x_1 F_i^A(x_1, p_T^2, \vec{r}, z) x_2 F_j^B(x_2, p_T^2, \vec{b} - \vec{r}, z') \\ &\quad \times \frac{\epsilon(y)p_T}{1 + \delta_{kl}} \left[\delta_{fk} \frac{d\hat{\sigma}^{ij \rightarrow kl}}{dt} (\hat{t}, \hat{u}) + \delta_{fl} \frac{d\hat{\sigma}^{ij \rightarrow kl}}{dt} (\hat{u}, \hat{t}) \right]. \end{aligned} \quad (1)$$

Identical particles in the final state are accounted for by the factor $1/(1 + \delta_{kl})$. The ratio of the NLO to LO jet cross sections, K_{jet} , indicates the size of the NLO corrections. A

*This work was supported in part by the Director, Office of Energy Research, Division of Nuclear Physics of the Office of High Energy and Nuclear Physics of the U. S. Department of Energy under Contract No. DE-AC03-76SF0098.

conservative $K_{\text{jet}} = 1$ [5] gives a lower limit on minijet production. The cutoff p_0 is the lowest p_T scale at which perturbative QCD is valid.

The nuclear parton densities, F_i^A , are assumed to be the product of the nucleon density in the nucleus $\rho_A(\vec{r}, z)$, the nucleon parton density $f_i^N(x, Q^2)$, and a shadowing function $S^i(A, x, Q^2, \vec{r}, z)$ where A is the atomic mass number, x is the parton momentum fraction, Q^2 is the interaction scale, and \vec{r} and z are the transverse and longitudinal location of the parton so that $F_i^A(x, Q^2, \vec{r}, z) = \rho_A(\vec{r}, z)S^i(A, x, Q^2, \vec{r}, z)f_i^N(x, Q^2)$. In the absence of nuclear modifications, $S^i(A, x, Q^2, \vec{r}, z) \equiv 1$. If the nuclear structure functions are homogeneous, then the spatial effects factorize and $\overline{E}_T^f(b, p_0)$ is proportional to the number of nucleon-nucleon collisions, $T_{AB}(b)$. We have calculated our results with GRV 94 LO [6] and MRST LO [7] parton distributions. The GRV low x gluon density is larger than the MRST and produces strikingly different results at LHC while the RHIC results are rather similar. We use three different parameterizations of shadowing, all based on nuclear deep inelastic scattering. The first parameterization, $S_1(A, x)$, treats quarks, antiquarks, and gluons identically without Q^2 evolution [8]. The others evolve with Q^2 and conserve baryon number and total momentum. The second, $S_2^i(A, x, Q^2)$, modifies the valence quarks, sea quarks and gluons separately and includes Q^2 evolution for $Q_0 = 2 < Q < 10$ GeV [9]. The third, $S_3^i(A, x, Q^2)$, evolves each parton type separately above $Q_0 = 1.5$ GeV [10]. We have studied the spatial dependence of shadowing using two parameterizations. If shadowing is proportional to the local density [3,11],

$$S_{\text{WS}}^i = S^i(A, x, Q^2, \vec{r}, z) = 1 + N_{\text{WS}}[S^i(A, x, Q^2) - 1] \frac{\rho_A(\vec{r}, z)}{\rho_0}, \quad (2)$$

where N_{WS} is chosen so that $(1/A) \int d^2r dz \rho_A(\vec{r}, z) S_{\text{WS}}^i = S^i$. If instead, shadowing arises due to multiple interactions of the incident parton, shadowing should be proportional to the path length of the parton through the nucleus,

$$S_{\text{R}}^i(A, x, Q^2, \vec{r}, z) = \begin{cases} 1 + N_{\text{R}}(S^i(A, x, Q^2) - 1) \sqrt{1 - (r/R_A)^2} & r \leq R_A \\ 1 & r > R_A \end{cases}. \quad (3)$$

The normalization, N_{R} , obtained after averaging over $\rho_A(\vec{r}, z)$, is slightly larger than N_{WS} . In both cases, at distances much greater than R_A , the nucleons behave as free particles while in the center of the nucleus, the modifications are larger than the average value S^i . We have also studied inhomogeneous shadowing assuming that shadowing is proportional to the path length through the nucleus and find that the central shadowing is somewhat stronger than with S_{WS}^i in Eq. (2).

The effect of the inhomogeneous shadowing, S_{WS}^i in Eq. (2), on $\overline{E}_T^f(b)$, calculated with the GRV 94 LO parton densities, is shown in Fig. 1 for CMS and STAR. The CMS and ALICE ratios are similar as are the STAR and PHENIX results. When x lies in the shadowing region, central collisions are more shadowed than the average. In the antishadowing region, central collisions are more antishadowed than the average. When $b \sim R_A$, the homogeneous and inhomogeneous shadowing are approximately equal. When $b \sim 2R_A$, shadowing/antishadowing is significantly reduced. As b increases further, $S = 1$ is approached asymptotically. When inhomogeneous shadowing is assumed to be proportional to S_{R}^i , Eq. (3), we find stronger shadowing at low impact parameter and a somewhat faster approach to $S = 1$ at large b .

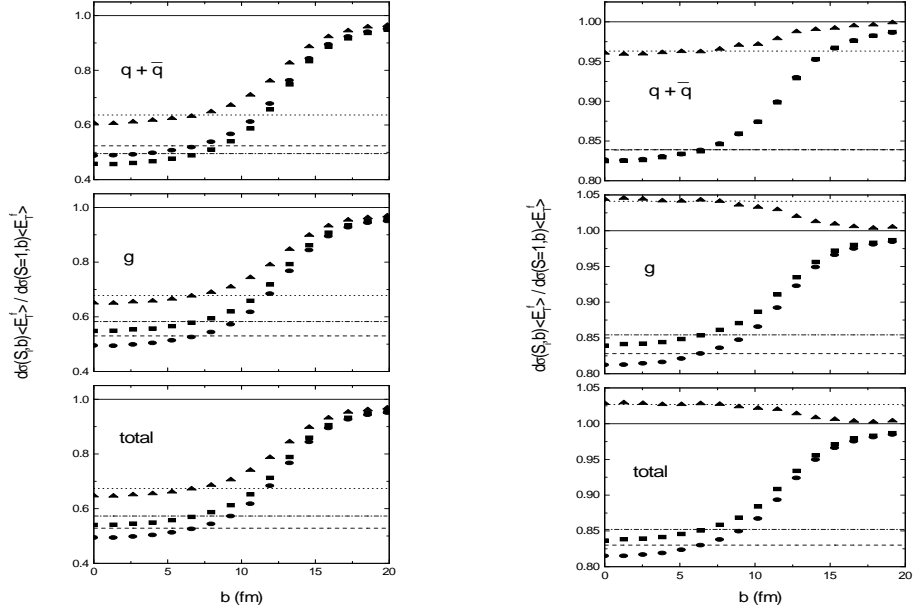


Figure 1. The impact parameter dependence of the first E_T moment, compared to that with $S = 1$ in CMS, $|y_{\max}| \leq 2.4$, at the LHC (left) and in STAR, $|y_{\max}| \leq 0.9$, at RHIC (right) calculated with the GRV 94 LO distributions and $p_0 = 2$ GeV. The upper plot shows the ratio for quarks and antiquarks, the middle plot is the gluon ratio and the lower plot is for the total. The horizontal lines show the homogeneous shadowing results: dashed for S_1 , dot-dashed for S_2 , and dotted for S_3 . The inhomogeneous shadowing results using S_{WS}^i for S_1 , circles, S_2 , squares, and S_3 , triangles are also shown [12].

We assume that the transverse energy distribution, $d\sigma/dE_T$, can be approximated by the Gaussian [5]

$$\frac{d\sigma}{dE_T} = \int \frac{d^2b}{\sqrt{2\pi\sigma_E^2(b)}} \exp\left(-\frac{[E_T - \bar{E}_T(b)]^2}{2\sigma_E^2(b)}\right), \quad (4)$$

The total E_T distribution is a convolution of the hard and soft components with mean and standard deviation

$$\bar{E}_T(b) = \sum_f \bar{E}_T^f(b) + T_{AB}(b)\epsilon_0 \quad \sigma_E^2(b) = \sum_f \bar{E}_T^2 - \frac{\bar{E}_T^H}{\sigma_H^2(p_0)} + T_{AB}(b) \left(\epsilon_1 - \frac{\epsilon_0^2}{\sigma_{pp}^S} \right). \quad (5)$$

The E_T distributions are shown for CMS and STAR in Fig. 2. At the LHC, 90% of the average E_T comes from the hard component, causing the maximum E_T to be halved due to shadowing. In fact, the low x gluon density is high enough for the incoming gluon to have multiple hard collisions, up to 5 in central collisions with no shadowing, as it traverses the nucleus when the GRV 94 LO distributions are used. In contrast, an incoming quark has at most 1 collision. Similar results with MRST LO distributions typically halve the hard E_T and significantly reduce gluon multiple scattering. Gluons suffer 1.4-2 hard collisions

while quarks scatter less than once [12]. At RHIC, since the hard and soft components are comparable, the maximum E_T is shifted by only $\sim 7\%$ when shadowing is included. Indeed, for S_3 , the maximum E_T is slightly increased. Thus shadowing significantly affects the initial conditions at LHC but not at RHIC. Ref. [12] gives more details and discusses inhomogeneous shadowing effects on J/ψ and Drell-Yan production.

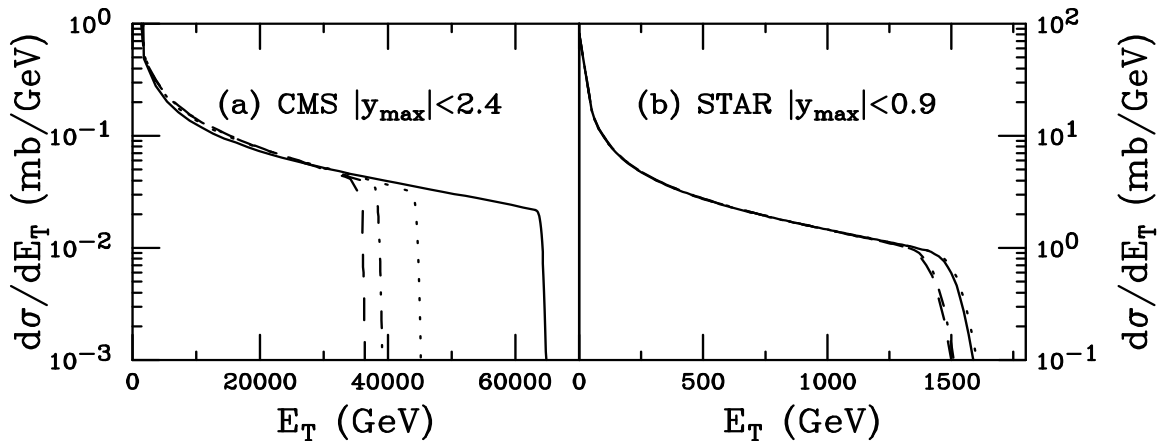


Figure 2. The E_T distribution predicted for CMS, $|y_{\max}| \leq 2.4$, at the LHC and STAR, $|y_{\max}| \leq 0.9$, at RHIC calculated with the GRV 94 LO distributions and $p_0 = 2$ GeV. The homogeneous shadowing results for all b are: no shadowing (solid), S_1 (dashed), S_2 (dot-dashed), and S_3 (dotted). Modified from Ref. [12].

REFERENCES

1. J.J. Aubert *et al.*, Nucl. Phys. **B293** 740, (1987); M. Arneodo, Phys. Rep. **240** 301, (1994).
2. T. Kitagaki *et al.*, Phys. Lett. **214**, 281 (1988).
3. V. Emel'yanov, A. Khodinov, S.R. Klein and R. Vogt, Phys. Rev. **C56**, 2726 (1997).
4. K.J. Eskola and M. Gyulassy, Phys. Rev. **C47** 2329, (1993).
5. K.J. Eskola and K. Kajantie, Z. Phys. **C75** 515, (1997);
6. M. Glück, E. Reya, and A. Vogt, Z. Phys. **C67** 433, (1995).
7. A.D. Martin, R.G. Roberts, and W.J. Stirling, and R.S. Thorne, Eur. Phys. J. **C4** (1998) 463; Phys. Lett. **B443** (1998) 301.
8. K.J. Eskola, J. Qiu, and J. Czyzewski, private communication.
9. K.J. Eskola, Nucl. Phys. **B400** 240, (1993).
10. K.J. Eskola, these proceedings.
11. V. Emel'yanov, A. Khodinov, S.R. Klein and R. Vogt, Phys. Rev. Lett. **81**, 1801 (1998).
12. V. Emel'yanov, A. Khodinov, S.R. Klein and R. Vogt, LBNL-42900.